S_NAr Reactions of 1-Halo-2,4-dinitrobenzenes with Alkali-Metal Ethoxides: Differential Stabilization of Ground State and Transition State Determines Alkali-Metal Ion Catalysis or Inhibition

Kiyull Yang,[†,*] Min-Young Kim,[‡] and Ik-Hwan Um[‡,*]

[†]*Department of Chemistry Education, Gyeongsang National University, Jinju 660-701, Korea.*
**E-mail: kyang@gnu.ac.kr*
[‡]*Department of Chemistry and Nano Science, Ewha Womans University, Seoul 120-750, Korea.*
**E-mail: ihum@ewha.ac.kr*
Received February 26, 2015, Accepted March 17, 2015, Published online June 24, 2015

A kinetic study on S_NAr reactions of 1-halo-2,4-dinitrobenzenes (**6a–6d**) with alkali-metal ethoxides (EtOM; M = Li, Na, K and 18-crown-6-ether-complexed K) is reported. The plots of pseudo-first-order rate constant (k_{obsd}) vs. [EtOM] curve upward or downward depending on the size of M^+ ions. The reactions are catalyzed or inhibited by the M^+ ions, *e.g.*, the large K^+ ion complexed by 18-crown-6-ether (18C6) acts as a catalyst while the small Li^+ and Na^+ ions behave as an inhibitor. Reactivity of **6a–6d** toward EtOM decreases linearly as the halide ion becomes less basic regardless of the size of M^+ ions, indicating that expulsion of the leaving group occurs after the rate-determining step (RDS). Thus, the reactions have been proposed to proceed through a stepwise mechanism with formation of a Meisenheimer complex being the RDS. Computational studies using B3LYP density functional theory have revealed that Mulliken charge density of the electrophilic center decreases as the halogen atom becomes less electronegative. Thus, it has been concluded that the S_NAr reactivity of **6a–6d** toward EtOM is governed by electrophilicity of the reaction center but not by nucleofugality of the leaving group. A π-complexed transition-state structure has been proposed to account for the experimental and computational results.

Keywords: S_NAr reaction, Alkali-metal ion catalysis or inhibition, Electrophilicity, Nucleofugality

Introduction

Metal ions have often been reported to act as a Lewis acid catalyst in nucleophilic substitution reactions of various esters.[1–10] Reactions involved multivalent metal ions (e.g., Mg^{2+}, Mn^{2+}, Zn^{2+}, La^{3+}, Eu^{3+}, Co^{3+}, etc.) have intensively been carried out due to their great Lewis acidity.[1–5] In contrast, studies on reactions involved alkali-metal ions (*e.g.*, Li^+, Na^+, and K^+) have attracted much less attention,[6–10] although alkali-metal ions are ubiquitous in nature and are known to play important roles in biological processes (*e.g.*, Na^+/K^+ pump in mammalian cells).[11]

Buncel and his coworkers initiated a systematic study on nucleophilic substitution reaction of 4-nitrophenyl diphenylphosphinate (**1a**) with alkali-metal ethoxides (EtOM; M = Li, Na, K) in anhydrous ethanol.[6a] They found that M^+ ions catalyze the reaction and the catalytic effect increases with decreasing size of M^+ ions (*i.e.*, $K^+ < Na^+ < Li^+$), but the catalytic effects disappeared in the presence of complexing agents such as 18-crown-6-ether (18C6) for K^+ ion, 15-crown-5-ether (15C5) for Na^+ ion, and [2,1,1]-cryptand for Li^+ ion.[6a] On the contrary, we have shown that the corresponding reaction of 4-nitrophenyl diphenylphosphinothioate (**1b**, a thio analog of **1a**) is strongly inhibited by Li^+ ion but is catalyzed by 18C6-crowned K^+ ion.[7a] Thus, the reactions of **1a** and **1b** have been proposed to proceed through a four-membered cyclic transition state (TS) as modeled by TS_1.[7a]

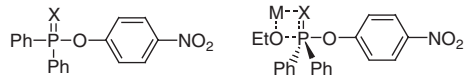

X = O (**1a**), S (**1b**) TS_1

We have also reported that M^+ ions catalyze reactions of 4-nitrophenyl X-substituted-benzenesulfonates (**2**) and Y-substituted-phenyl benzenesulfonates (**3**) with EtOM.[7b] Interestingly, the catalytic effect increased on changing the substituent X in the benzenesulfonyl moiety from a strong electron-withdrawing group (EWG) to a strong electron-donating group (EDG), but was nearly independent of the electronic nature of the substituent Y in the leaving group. Thus, M^+ ions have been reported to catalyze the reactions of **2** and **3** by increasing electrophilicity of the reaction center through TS_2 rather than by enhancing nucleofugality of the leaving group via TS_3.[7b]

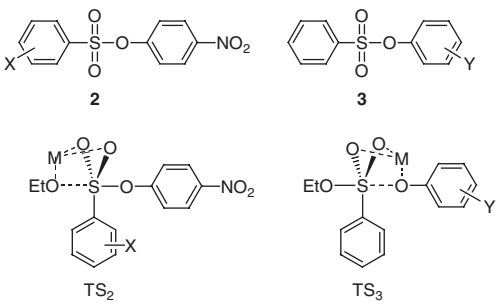

In contrast, M^+ ions have been reported to catalyze nucleophilic substitution reactions of 2-pyridyl benzoate (**4a**) with EtOM by increasing nucleofugality of the leaving group.[10] We have shown that M^+ ions strongly catalyze the reaction of **4a**, but not the corresponding reaction of 4-pyridyl benzoate (**4b**, an isomer of **4a**).[10] One might expect that the reactions of **4a** would proceed through a six-membered cyclic TS as modeled by TS_4, in which M^+ ion could increase nucleofugality of the leaving group. However, such a cyclic complex is structurally not possible for the corresponding reactions of **4b**. Thus, M^+ ions have been concluded to catalyze the reactions of **4a** by increasing nucleofugality of the leaving group through TS_4.[10]

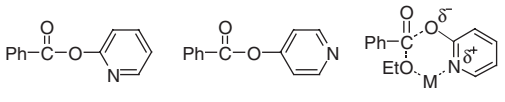

4a **4b** TS_4

Effects of M^+ ions on S_NAr reactions of various activated aromatic halides have also been investigated including theoretical studies.[9b,c,12] Jones *et al.* have carried out computational studies using DFT methods on S_NAr reactions of mono-, di-, and tri-activated fluorobenzenes (**5**) with alkali-metal cresolates (Scheme 1).[12] They have concluded that M^+ ions ($M^+ = Li^+$, Na^+ and K^+) facilitate expulsion of the leaving group through a four-membered cyclic TS as modeled by TS_5 in Scheme 1.[12]

We have previously carried out a kinetic study on S_NAr reactions of 1-fluoro-2,4-dinitrobenzene (**6a**) and 1-chloro-2,4-dinitrobenzene (**6b**) with EtOM (M = Li, Na, and K) in anhydrous ethanol.[9c] We have shown that the reactions are inhibited by Li^+ ion, but are catalyzed by 18C6-crowned K^+ ion.[9c] Our kinetic study has now been extended to S_NAr reactions of 1-bromo-2,4-dinitrobenzene (**6c**) and 1-iodo-2,4-dinitrobenzene (**6d**) with EtOM (M = Li, Na and K) in anhydrous ethanol to obtain further information on the role of M^+ ions together with the reaction mechanism (Scheme 2). We have also carried out computational studies on Mulliken electron density of the electrophilic center of **6a–6d** to give further credence to the proposal based on the experimental results.

Results and Discussion

The kinetic study was carried out spectrophotometrically under pseudo-first-order conditions in which the EtOM concentration was in large excess over the substrate concentration. All the reactions in this study obeyed pseudo-first-order kinetics. Pseudo-first-order rate constants (k_{obsd}) were calculated from equation, $\ln (A_\infty - A_t) = -k_{obsd}t + C$. The uncertainty in the k_{obsd} values was estimated to be less than ±3% from replicate runs. As shown in Figure 1, the plots of k_{obsd} vs. [EtOM] for the reactions of **6c** and **6d** curve downward or upward depending on the size of alkali-metal ions. The second-order rate constants for the reactions with the dissociated EtO^- and ion-paired EtOM (*i.e.*, k_{EtO-} and k_{EtOM}, respectively) were calculated from the ion-pairing treatment of the kinetic data, and are summarized in Table 1. The Mulliken charge density q values calculated for the electrophilic center of **6a–6d** are summarized in Table 2. Detailed kinetic conditions and results (*i.e.*, the k_{obsd} data as a function of [EtOM]) are summarized in Tables S1–S8 in the Supporting Information.

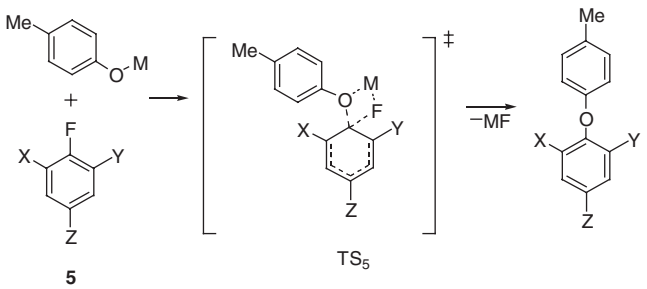

5 TS_5

Scheme 1. S_NAr reactions of **5** with alkali-metal cresolates.

M^+ Ion Catalysis and Inhibition. Figure 1 shows that the reactivity of EtOM toward substrates **6c** and **6d** increases as the size of M^+ ions increases, *i.e.*, the k_{obsd} value at a given concentration of EtOM increases in the order EtOLi < EtONa < EtOK < EtOK/18C6. It is also noted that the plots of k_{obsd} vs. [EtOM] for the reactions of **6c** and **6d** curve downward or upward depending on size of M^+ ions, i.e., downward curvature for the reactions with EtOLi and EtONa but upward curvature for those with EtOK/18C6. The fact that the reactivity of EtOM is dependent on the size of M^+ ions indicates that M^+

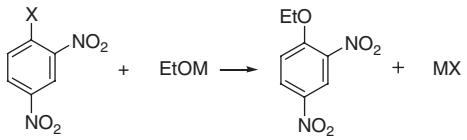

X = F (**6a**), Cl (**6b**), Br (**6c**), I (**6d**).

M = Li, Na, K, 18C6-crowned-K.

Scheme 2. Reactions of **6a–6d** with alkali-metal ethoxides.

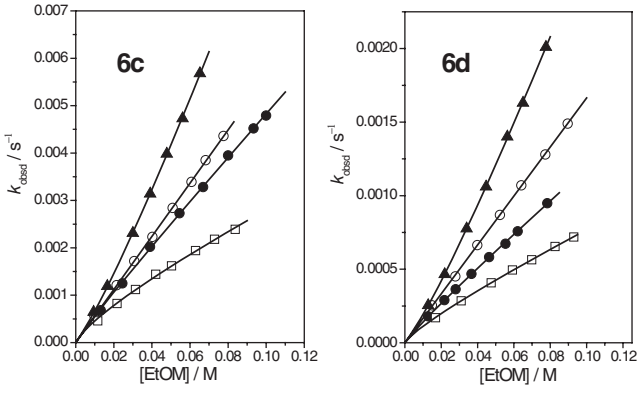

Figure 1. Plots of k_{obsd} vs. [EtOM] for the S_NAr reactions of 1-bromo-2,4-dinitrobenzene (**6c**) and 1-iodo-2,4-dinitrobenzene (**6d**) with EtOLi (□), EtONa (●), EtOK (○), and EtOK/18C6 (▲) in anhydrous EtOH at 25.0 ± 0.1 °C. [18C6]/[EtOK] = 2.0.

ions are involved in the TS as well as in the ground state (GS). Thus, one can suggest that M^+ ions behave either as an inhibitor or as a catalyst in the current S_NAr reactions depending on relative stabilization of the GS and TS.

Pechanec *et al*. reported that alkali-metal ethoxides in anhydrous ethanol exist as dissociated EtO^- and ion-paired EtOM when [EtOM] < 0.1 M.[13] It is noted that the concentration of EtOM used in this study is lower than 0.1 M. Therefore, substrates **6a–6d** would react with both the dissociated EtO^- and ion-paired EtOM with rate constants k_{EtO-} and k_{EtOM}, respectively, as shown in Scheme 3.

Thus, one can derive Eq. (1) on the basis of the reactions proposed in Scheme 3. Under pseudo-first-order kinetic conditions (*e.g*., [EtOM] >> [**6c** or **6d**]), k_{obsd} can be expressed as Eq. (2). It is noted that the dissociation constant $K_d = [EtO^-]_{eq}[M^+]_{eq}/[EtOM]_{eq}$ and $[EtO^-]_{eq} = [M^+]_{eq}$ at equilibrium. Thus, Eq. (2) can be converted to Eq. (3). The concentrations of $[EtO^-]_{eq}$ and $[EtOM]_{eq}$ can be calculated from the reported K_d values of EtOM and the initial concentration [EtOM] using Eqs. (4) and (5).

$$\text{Rate} = k_{EtO^-}[EtO^-]_{eq}[\mathbf{6c}-\mathbf{6d}] + k_{EtOM}[EtOM]_{eq}[\mathbf{6c}-\mathbf{6d}] \quad (1)$$

$$k_{obsd} = k_{EtO^-}[EtO^-]_{eq} + k_{EtOM}[EtOM]_{eq} \quad (2)$$

$$k_{obsd}/[EtO^-]_{eq} = k_{EtO^-} + k_{EtOM}[EtO^-]_{eq}/K_d \quad (3)$$

$$[EtOM] = [EtO^-]_{eq} + [EtOM]_{eq} \quad (4)$$

$$[EtO^-]_{eq} = \left[-K_d + \left(K_d^2 + 4K_d[EtOM]\right)^{1/2}\right]/2 \quad (5)$$

Table 1. Summary of second-order rate constants for the S_NAr reactions of 1-halo-2,4-dinitrobenzenes (**6a–6d**) with ion-paired EtOM and dissociated EtO^- (*i.e*., $k_{EtOM}/M^{-1}s^{-1}$ and $k_{EtO-}/M^{-1}s^{-1}$, respectively) in anhydrous ethanol at 25.0 ± 0.1 °C[a].

	6a	6b	6c	6d
k_{EtOLi}	30.6	0.0394	0.0183	0.00547
k_{EtONa}	68.5	0.0693	0.0441	0.00990
k_{EtOK}	91.0	0.109	0.0554	0.0166
$k_{EtOK/18C6}$	182	0.228	0.128	0.0387
k_{EtO-}	63.2	0.0857	0.0593	0.0164

[a] The data for the reactions of **6a** and **6b** were taken from Ref. 9c. [18C6]/[EtOK] = 2.0.

Table 2. Mulliken charge density (q) of the electrophilic center of 1-halo-2,4-dinitrobenzenes (**6a–6d**) computed by B3LYP/3-21G* basis sets.

Substrate	q
6a	0.3519
6b	0.2998
6c	0.2752
6d	0.2708

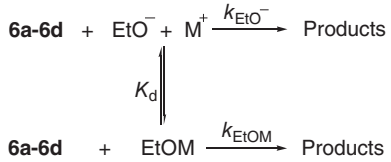

Scheme 3. Reactions of **6a–6d** with the dissociated EtO^- and ion-paired EtOK.

The plot of $k_{obsd}/[EtO^-]_{eq}$ vs. $[EtO^-]_{eq}$ would be linear if the current reaction proceeds as proposed in Scheme 3. In fact, the plots shown in Figure 2 exhibit excellent linearity with a common intercept, indicating that the derived equations based on the reactions shown in Scheme 3 are correct. Accordingly, the k_{EtO-} and k_{EtOM}/K_d values were calculated from the intercept and the slope of the linear plots, respectively. The k_{EtOM} value was calculated from the above k_{EtOM}/K_d values and the K_d values for EtOM reported in literature.[8a,14] The k_{EtO-} and k_{EtOM} values calculated in this way for the reactions of **6c** and **6d** are summarized in Table 1 together with those reported previously for the corresponding reactions of **6a** and **6b** for comparison.

Comparison of Experimental and Computational Studies. As shown in Table 1, the reactivity of EtOM toward substrates **6c** and **6d** increases in the order EtOLi < EtONa < EtOK < EtO^- < EtOK/18C6, indicating that the ion-paired species EtOM (except EtOK/18C6) are less reactive than the dissociated EtO^- toward **6c** and **6d**. This is slightly different from the reactivity order for the corresponding reactions of **6a** and **6b** (*i.e*., EtOLi < EtO^- < EtONa < EtOK < EtOK/18C6 for the reaction of **6a**, and EtOLi < EtONa < EtO^- < EtOK < EtOK/18C6 for the reaction of **6b**).

Jones *et al*. have recently carried out computational studies on S_NAr reactions of mono-, di-, and tri-activated fluorobenzenes (**5**) with alkali-metal cresolates (Scheme 1 in the *Introduction* section).[12] According to their calculations using DFT methods, the activation energy increased as size of M^+ ions

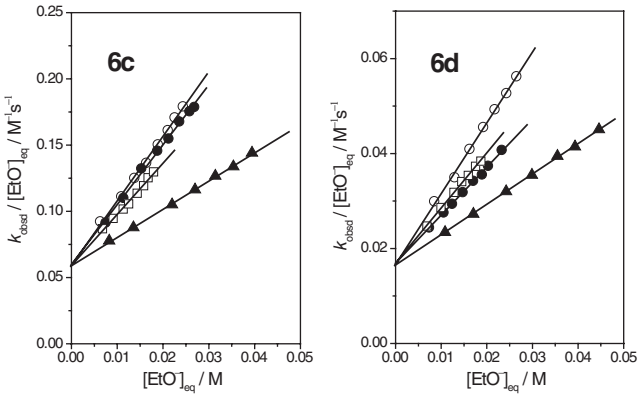

Figure 2. Plots of $k_{obsd}/[EtO^-]_{eq}$ vs. $[EtO^-]_{eq}$ for the S_NAr reactions of 1-bromo-2,4-dinitrobenzene (**6c**) and 1-iodo-2,4-dinitrobenzene (**6d**) with EtOLi (□), EtONa (●), EtOK (○), and EtOK/18C6 (▲) in anhydrous EtOH at 25.0 ± 0.1 °C. [18C6]/[EtOK] = 2.0.

decreased.[12] They have also reported that M^+ ions increase the energy barrier (*i.e.*, a decrease in reactivity) due to formation of stable reactant complexes upon interaction with the fluorobenzenes.[12] Nevertheless, M^+ ions have been concluded to facilitate expulsion of the leaving group by forming a four-membered cyclic TS as modeled by TS_5.[12]

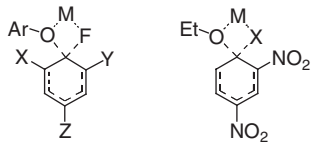

TS_5 TS_6

It is notable that our experimental results appear to be consistent with the computational results reported by Jones *et al.*, because M^+ ions (except 18C6-crowned K^+ ion) inhibit the reactions of **6a–6d**, and the inhibitory effect increases as size of M^+ ions decreases. Accordingly, one might suggest that the current S_NAr reactions proceed also through TS_6, in which M^+ ion would increase nucleofugality of the leaving group. *However, the enhanced nucleofugality through* TS_6 *cannot accelerate the overall reaction rate if expulsion of the leaving group occurs after the rate-determining step (RDS).* Thus, detailed information on the reaction mechanism including the RDS is necessary to investigate TS structure in the current S_NAr reactions.

Deduction of Reaction Mechanism. S_NAr reactions have generally been reported to proceed through a stepwise mechanism with a Meisenheimer complex in which the RDS is dependent on reaction conditions (*e.g.*, nature of reaction medium, type of nucleophile, etc.).[15–18] S_NAr reactions of **6a** with a series of cyclic secondary amines have been reported to proceed through a stepwise mechanism with a zwitterionic Meisenheimer complex, in which the RDS changes from formation of the Meisenheimer complex to its breakdown as the reaction medium varies from H_2O to an aprotic solvent MeCN.[15c] In contrast, formation of a Meisenheimer complex has been suggested to be the RDS for S_NAr reactions of **6a** with primary amines in MeCN[15b] and for S_NAr reactions of 1-(Y-substituted-phenoxy)-2,4-dinitrobenzenes with EtOM in anhydrous ethanol regardless of the nature of the substituent Y in the leaving group.[9b]

To deduce the reaction mechanism, Brønsted-type plots for the reactions of **6a–6d** with EtOK/18C6 have been constructed in Figure 3. The plots exhibit excellent linear correlations. Interestingly, the logarithmic rate constants (*i.e.*, log $k_{EtOK/18C6}$ and log k_{EtO^-}) increase linearly as basicity of the leaving halide ions increases. This is not possible if expulsion of the leaving group is involved in the RDS. Thus, one can conclude that expulsion of the leaving group occurs after the RDS.

Table 1 shows that the reactivity of **6a–6d** toward EtOM decreases as the size of the halogen atom increases. This appears to be consistent with the report that steric hindrance affects S_NAr reactivity of 1-(X-substituted-phenoxy)-2,4,6-trinitrobenzenes toward substituted-anilines in acetonitrile.[19] Furthermore, Figure 4 demonstrates that the logarithmic rate constants decrease linearly as 1/radius of the halide ion decreases. Accordingly, one might suggest that steric hindrance is also responsible for the reactivity order found in the current S_NAr reactions.

However, if steric hindrance is an important factor that controls S_NAr reactivity of **6a–6d**, k_{EtOM} would decrease as the size of M^+ ions increases (*e.g.*, EtOLi > EtONa > EtOK > EtOK/18C6). This is because steric hindrance would be more significant as the size of M^+ ions increases. In fact, k_{EtOM} increases with increasing the size of M^+ ions (Table 1). Furthermore, Figure S1 demonstrates that the reactivity of EtOM increases linearly with decreasing 1/ionic radius of M^+ ions. This is not possible if steric hindrance affects the S_NAr reactivity in this study. Thus, one can suggest that other than steric hindrance (*e.g.*, nature of the reaction mechanism) is also responsible for the reactivity order shown in Table 1.

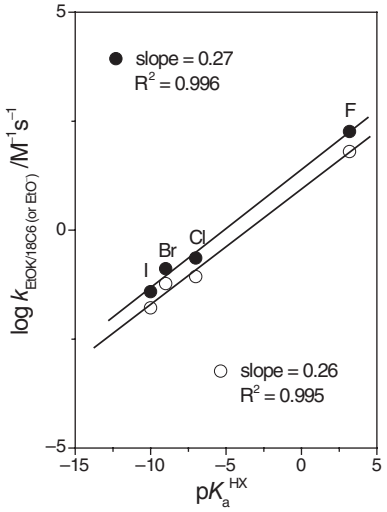

Figure 3. Brønsted-type plots for the S_NAr reactions of 1-halo-2,4-dinitrobenzenes (**6a–6d**) with EtOK under the presence of 18C6 in anhydrous ethanol at 25.0 ± 0.1 °C. log $k_{EtOK/18C6}$ vs. pK_a of HX (●) and log k_{EtO^-} vs. pK_a of HX (○).

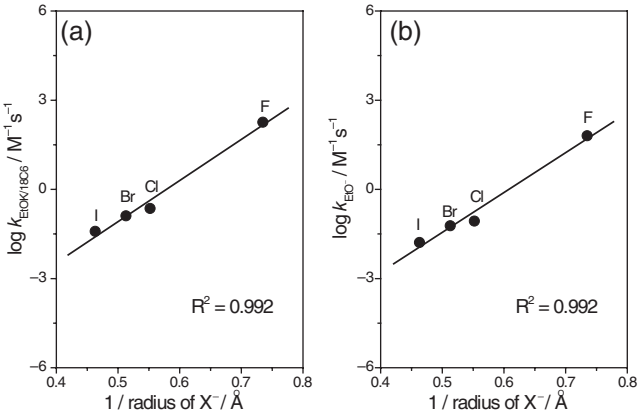

Figure 4. Effect of halide-ion size on S_NAr reactivity of 1-halo-2,4-dinitrobenzenes (**6a–6d**) toward EtOK/18C6 (**a**) and dissociated EtO^- (b). The size of X^- ions was taken from Ref. 23a.

To shed more light on the reaction mechanism, log $k_{EtOK/18C6}$ and log k_{EtO^-} values for the reactions of **6a–6d** have been correlated with electronegativity (EN) of the halogen atoms. As shown in Figure 5, the logarithmic rate constants increase linearly with increasing the EN of the halogen atoms. It is apparent that electrophilicity of the reaction center would increase as the halogen atom in **6a–6d** becomes more electronegative (*i.e.*, I < Br < Cl < F). Thus, the linear plots shown in Figure 5 suggest that the S_NAr reactivity of **6a–6d** toward EtOM is governed by electrophilicity of the reaction center.

To examine validity of the above argument, Mulliken charge density of the reaction sites has been calculated using the B3LYP density functional theory with 3-21G∗ basis sets implemented in Gaussian 03 package.[20] Table 2 shows that the Mulliken charge density of the reaction center (q) decreases as the halogen atom in **6a–6d** becomes less electronegative. Furthermore, as shown in Figure S2, the calculated q value exhibits a linear correlation with the rate constants (*i.e.*, log $k_{EtOK/18C6}$ and log k_{EtO^-}). This is consistent with the argument that reactivity of **6a–6d** is governed by electrophilicity of the reaction center. Thus, one can conclude that the S_NAr reactions of **6a–6d** with EtOM proceed through a stepwise mechanism with a Meisenheimer complex, in which expulsion of the leaving group occurs after the RDS.

TS Structure and Role of M^+ Ions. As expulsion of the leaving group occurs after the RDS, one can exclude a possibility that M^+ ions catalyze the current S_NAr reaction by increasing nucleofugality of the leaving group through the four-membered cyclic TS as modeled by TS_6. To account for the kinetic results, the S_NAr reactions of **6a–6d** with EtOM are proposed to proceed through a π-complexed TS (*i.e.*, TS_7) as shown in Scheme 4. It is noted that TS_7 is similar to the stable π-adducts reported previously for the reactions of transition-metal ions with aromatic systems (*e.g.*, ferrocene, uranocene, etc.)[21] and for S_NAr reactions of 1-(Y-substituted-phenoxy)-2,4-dinitrobenzenes with EtOM.[9b]

One might expect that the polarizable π-electrons in the benzene ring of TS_7 would interact strongly with the large 18C6-crowned K^+ ion but weakly with a small M^+ ion such as Li^+ or Na^+ ion on the basis of the Hard-Soft Acids and Bases (HSAB) principle.[22] Thus, stabilization of the TS through TS_7 would increase with increasing the size of M^+ ions (*i.e.*, $Li^+ < Na^+ < K^+ <$ 18C6-crowned K^+). In contrast, the GS of EtOM would be stabilized mainly through ion-pairing interactions between EtO^- and M^+ ions. Since ion-pairing interaction would increase with increasing charge density of M^+ ions, the GS of the ion-paired EtOM would be more stabilized as the size of M^+ ions decreases (*i.e.*, EtOK/18C6 < EtOK < EtONa < EtOLi). This idea is in accord with the kinetic results that the S_NAr reactions of **6c** and **6d** are inhibited by M^+ ions (except 18C6-crowned K^+ ion) and the inhibitory effect increases as the size of M^+ ions decreases. In contrast, the catalysis by the 18C6-crowned K^+ ion indicates that TS stabilization through TS_7 outweighs GS stabilization via ion-pairing interactions between EtO^- and 18C6-crowned K^+ ion.

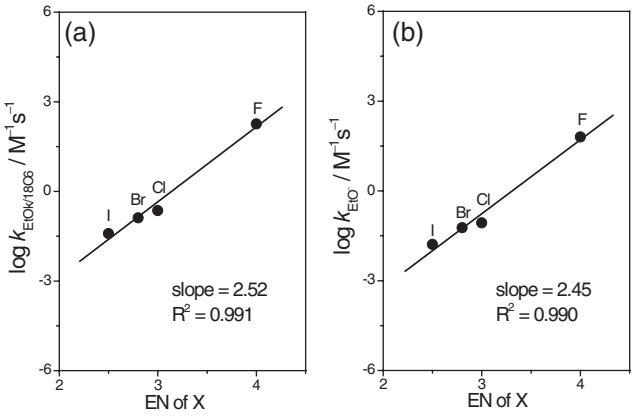

Figure 5. Plots showing effect of EN of halogen atom X on reactivity of 1-halo-2,4-dinitrobenzenes (**6a–6d**) toward EtOK/18C6 (**a**) and dissociated EtO^- (b). The EN values of halogen atom X were taken from Ref. 23b.

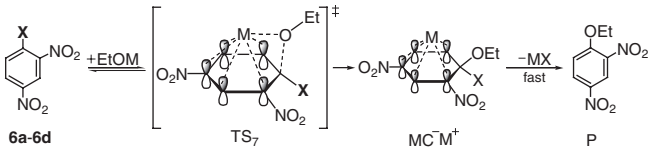

Scheme 4. Proposed reaction mechanism.

Conclusion

The current study has led us to conclude the following: (1) The k_{EtOM} value for the reactions of **6c** and **6d** increases in the order $k_{EtOLi} < k_{EtONa} < k_{EtOK} < k_{EtO^-} < k_{EtOK/18C6}$, indicating that the ion-paired species (except EtOK/18C6) are less reactive than the dissociated EtO^-. (2) Reactivity of **6a–6d** increases with increasing leaving-group basicity, implying that expulsion of the leaving group occurs after the RDS. (3) Reactivity of EtOM increases linearly with increasing the size of M^+ ions including 18C6-crowned K^+ ion, indicating that steric hindrance is not an important factor in the current S_NAr reactions. (4) The current reactions proceed through a π-complexed TS as modeled by TS_7. (5) Differential stabilization of the GS and TS determines M^+ ion catalysis or inhibition observed in the current S_NAr reactions. Inhibition by Li^+ and Na^+ ions indicates that GS stabilization through ion-pairing interactions between EtO^- and Li^+ (or Na^+) ion outweighs TS stabilization via TS_7. In contrast, the catalysis shown by 18C6-crowned K^+ implies that TS stabilization through TS_7 outweighs GS stabilization via ion-pairing interactions between EtO^- and 18C6-crowned K^+ ions.

Experimental Section

Materials. EtOM solutions were prepared by dissolving the respective alkali-metal in anhydrous ethanol under N_2 and stored in the refrigerator. The concentrations of EtOM were determined by titration with potassium hydrogen phthalate.

18-Crown-6-ether was recrystallized from acetonitrile and dried over P_2O_5 *in vacuo*. The anhydrous ethanol was further dried over magnesium and distilled under N_2 just before use. 1-Halo-2,4-dinitrobenzenes (**6a–6d**) and other chemicals were of the highest quality available.

Kinetics. Kinetic study was performed using a UV–Vis spectrophotometer equipped with a constant-temperature circulating bath. The reactions were followed by monitoring appearance of 1-ethoxy-2,4-dinitrobenzene at 310 nm. Pseudo-first-order conditions with the EtOM concentration at least 20 times greater than the substrate concentration were used. Generally, reactions were followed for 9–10 half-lives and k_{obsd} values were calculated using the equation, $\ln (A_\infty - A_t) = -k_{obsd}t + C$. The kinetic conditions and the k_{obsd} values are summarized in Tables S1–S8.

Product Analysis. 1-Ethoxy-2,4-dinitrobenzene was formed quantitatively and identified as one of the products by comparison of the UV–Vis spectrum after completion of the reaction with that of the authentic sample under the same reaction condition.

Acknowledgments. Publication cost of this paper was supported by the Korean Chemical Society.

Supporting Information. Additional supporting information is available in the online version of this article.

References

1. (a) M. N. Belzile, A. A. Neverov, R. S. Brown, *Inorg. Chem.* **2014**, *53*, 7916; (b) A. A. Neverov, L. D. Chen, S. George, D. Simon, C. I. Maxwell, R. S. Brown, *Can. J. Chem.* **2013**, *91*, 1139; (c) C. I. Maxwell, N. J. Mosey, R. S. Brown, *J. Am. Chem. Soc.* **2013**, *135*, 17209; (d) M. F. Mohamed, I. Sanchez-Lombardo, A. A. Neverov, R. S. Brown, *Org. Biomol. Chem.* **2012**, *10*, 631; (e) I. F. Barrera, C. I. Maxwell, A. A. Neverov, R. S. Brown, *J. Org. Chem.* **2012**, *77*, 4156.
2. (a) N. Mitic, K. S. Hadler, L. R. Gahan, A. C. Hengge, G. Schenk, *J. Am. Chem. Soc.* **2010**, *132*, 7049; (b) G. Feng, E. A. Tanifum, H. Adams, A. C. Hengge, *J. Am. Chem. Soc.* **2009**, *131*, 12771; (c) T. Humphry, S. Iyer, O. Iranzo, J. R. Morrow, J. P. Richard, P. Paneth, A. C. Hengge, *J. Am. Chem. Soc.* **2008**, *130*, 17858; (d) J. G. Zalatan, I. Catrina, R. Mitchell, P. K. Grzyska, P. J. O'Brien, D. Herschlag, A. C. Hengge, *J. Am. Chem. Soc.* **2007**, *129*, 9789; (e) A. G. Davies, *J. Chem. Soc. Perkin Trans.* **1997**, *1*, 2000.
3. (a) J. H. Lee, J. Park, M. S. Lah, J. Chin, J. I. Hong, *Org. Lett.* **2007**, *9*, 3729; (b) M. Livieri, F. Manicin, G. Saielli, J. Chin, U. Tonellato, *Chem. Eur. J.* **2007**, *13*, 2246; (c) M. Livieri, F. Mancin, U. Tonellato, J. Chin, *Chem. Commun.* **2004**, 2862.
4. (a) T. H. Fife, L. Chauffe, *Bioorg. Chem.* **2000**, *28*, 357; (b) T. H. Fife, R. Bembi, *J. Am. Chem. Soc.* **1993**, *115*, 11358; (c) T. H. Fife, M. P. Pujari, *J. Am. Chem. Soc.* **1990**, *112*, 5551; (d) W. S. Chei, H. Ju, J. Suh, *Bioorg. Med. Chem. Lett.* **2012**, *22*, 1533; (e) W. S. Chei, H. Ju, J. Suh, *J. Biol. Inorg. Chem.* **2011**, *16*, 511; (f) H. M. Kim, B. Jang, Y. E. Cheon, M. P. Suh, J. Suh, *J. Biol. Inorg. Chem.* **2009**, *14*, 151; (g) W. S. Chei, J. Suh, *Prog. Inorg. Chem.* **2007**, *55*, 79; (h) C. S. Jeung, J. B. Song, Y. H. Kim, J. Suh, *Bioorg. Med. Chem. Lett.* **2001**, *11*, 3061.
5. (a) J. I. Lee, *Bull. Korean Chem. Soc.* **2010**, *31*, 749; (b) J. I. Lee, *Bull. Korean Chem. Soc.* **2007**, *28*, 863; (c) S. Kim, J. I. Lee, *J. Org. Chem.* **1984**, *49*, 1712; (d) S. Kim, J. I. Lee, Y. K. Ko, *Tetrahedron Lett.* **1984**, *25*, 4943; (e) S. Kim, J. I. Lee, *J. Org. Chem.* **1983**, *48*, 2608.
6. (a) E. Buncel, E. J. Dunn, R. B. Bannard, J. G. Purdon, *J. Chem. Soc. Chem. Commun.* **1984**, 162; (b) E. J. Dunn, E. Buncel, *Can. J. Chem.* **1989**, *67*, 1440; (c) M. J. Pregel, E. J. Dunn, R. Nagelkerke, G. R. J. Thatcher, E. Buncel, *Chem. Soc. Rev.* **1995**, *24*, 449; (d) E. Buncel, R. Nagelkerke, G. R. J. Thatcher, *Can. J. Chem.* **2003**, *81*, 53; (e) R. Nagelkerke, G. R. J. Thatcher, E. Buncel, *Org. Biomol. Chem.* **2003**, *1*, 163; (f) E. Buncel, K. G. Albright, I. Onyido, *Org. Biomol. Chem.* **2004**, *2*, 601; (g) E. Buncel, K. G. Albright, I. Onyido, *Org. Biomol. Chem.* **2005**, *3*, 1468; (h) I. S. Koo, D. Ali, K. Yang, Y. Park, A. Esbata, G. W. van Loon, E. Buncel, *Can. J. Chem.* **2009**, *87*, 433.
7. (a) I. H. Um, Y. H. Shin, J. E. Park, J. S. Kang, E. Buncel, *Chem. Eur. J.* **2012**, *18*, 961; (b) I. H. Um, J. S. Kang, Y. H. Shin, E. Buncel, *J. Org. Chem.* **2013**, *78*, 490.
8. (a) I. H. Um, Y. H. Shin, S. E. Lee, K. Y. Yang, E. Buncel, *J. Org. Chem.* **2008**, *73*, 923; (b) I. H. Um, S. E. Jeon, M. H. Baek, H. R. Park, *Chem. Commun.* **2003**, 3016.
9. (a) I. H. Um, J. A. Seo, M. Mishima, *Chem. Eur. J.* **2011**, *17*, 3021; (b) I. H. Um, H. J. Cho, M. Y. Kim, E. Buncel, *Chem. Eur. J.* **2014**, *20*, 13337; (c) M. Y. Kim, G. H. Ha, I. H. Um, *Bull. Korean Chem. Soc.* **2014**, *35*, 2438.
10. J. I. Lee, J. S. Kang, S. I. Kim, I. H. Um, *Bull. Korean Chem. Soc.* **2010**, *31*, 2929.
11. (a) D. W. Martin, P. A. Mayes, V. W. Rodwell, D. K. Granner, *Harper's Review of Biochemistry*, 20th ed., Lange Medical Publications, Los Altos, CA, **1985**, p. 630; (b) H. Dugas, *Bioorganic Chemistry*, 2nd ed., Springer-Verlag, New York, **1989**, p. 284.
12. G. O. Jones, A. A. Somaa, J. M. O'Brien, H. Albishi, H. A. Al-Megren, A. M. Alabdulrahman, F. D. Alsewailem, J. L. Hedrick, J. E. Rice, H. W. Horn, *J. Org. Chem.* **2013**, *78*, 5436.
13. V. Pechanec, O. Kocian, J. Zavada, *Collect. Czech. Chem. Commun.* **1982**, *47*, 3405.
14. J. Barthel, J.-C. Justice, R. Z. Wachter, *Phys. Chem.* **1973**, *84*, 100.
15. (a) I. H. Um, M. Y. Kim, T. A. Kang, J. M. Dust, *J. Org. Chem.* **2014**, *79*, 7025; (b) I. H. Um, L. R. Im, J. S. Kang, S. S. Bursey, J. M. Dust, *J. Org. Chem.* **2012**, *77*, 9738; (c) I. H. Um, S. W. Min, J. M. Dust, *J. Org. Chem.* **2007**, *72*, 8797.
16. (a) N. El-Guesmi, T. Boubaker, F. Goumont, F. Terrier, *Org. Biomol. Chem.* **2008**, 6, 4041; (b) F. Terrier, E. Magnier, E. Kizilian, C. Wakselman, E. Buncel, *J. Am. Chem. Soc.* **2005**, 127, 5563; (c) F. Terrier, In *Nucleophilic Aromatic Displacement: The Influence of the Nitro Group*. Organic Nitro Chemistry Series, H. Feuer Ed., VCH, New York, **1991**; (d) F. Terrier, *Modern Nucleophilic Aromatic Substitution*, Wiley-VCH, Weinheim, **2013**, p. 57; (e) E. Buncel, M. R. Crampton, M. J. Strauss, F. Terrier, *Electron Deficient Aromatic– and Heteroaromatic–Base Interactions*, Elsevier, New York, **1984**.
17. (a) C. F. Bernasconi, *MTP Int. Rev. Sci. Org. Chem. Ser. One* **1973**, *3*, 33; (b) C. F. Bernasconi, *Acc. Chem. Res.* **1978**, *11*, 147; (c) C. W. Rees, B. Capon, *Annu. Rep. Prog. Chem.* **1962**, *59*, 207; (d) N. S. Nudelman, D. Palleros, *J. Org. Chem.* **1983**, *48*, 1607; (e) J. Hirst, *J. Phys. Org. Chem.* **1989**, *2*, 1.

18. (a) J. M. Dust, R. A. Manderville, *Can. J. Chem.* **1998**, *76*, 1019; (b) J. M. Dust, E. Buncel, *Can. J. Chem.* **1994**, *72*, 218; (c) J. M. Dust, E. Buncel, *Can. J. Chem.* **1991**, *69*, 978.
19. (a) C. Isanbor, T. A. Emokpae, *Int. J. Chem. Kinet.* **2010**, *42*, 37; (b) C. Isanbor, A. I. Babatunde, *J. Phys. Org. Chem.* **2009**, *22*, 1078; (c) T. A. Emokpae, N. V. Atasie, *Int. J. Chem. Kinet.* **2005**, *37*, 744.
20. M. J. Frisch, G. W. Trucks, H. B. Schlegel, G. E. Scuseria, M. A. Robb, J. R. Cheeseman, J. A. Montgomery, Jr., T. Vreven, K. N. Kudin, J. C. Burant, J. M. Millam, S. S. Iyengar, J. Tomasi, V. Barone, B. Mennucci, M. Cossi, G. Scalmani, N. Rega, G. A. Petersson, H. Nakatsuji, M. Hada, M. Ehara, K. Toyota, R. Fukuda, J. Hasegawa, M. Ishida, T. Nakajima, Y. Honda, O. Kitao, H. Nakai, M. Klene, X. Li, J. E. Knox, H. P. Hratchian, J. B. Cross, V. Bakken, C. Adamo, J. Jaramillo, R. Gomperts, R. E. Stratmann, O. Yazyev, A. J. Austin, R. Cammi, C. Pomelli, J. W. Ochterski, P. Y. Ayala, K. Morokuma, G. A. Voth, P. Salvador, J. J. Dannenberg, V. G. Zakrzewski, S. Dapprich, A. D. Daniels, M. C. Strain, O. Farkas, D. K. Malick, A. D. Rabuck, K. Raghavachari, J. B. Foresman, J. V. Ortiz, Q. Cui, A. G. Baboul, S. Clifford, J. Cioslowski, B. B. Stefanov, G. Liu, A. Liashenko, P. Piskorz, I. Komaromi, R. L. Martin, D. J. Fox, T. Keith, M. A. Al-Laham, C. Y. Peng, A. Nanayakkara, M. Challacombe, P. M. W. Gill, B. Johnson, W. Chen, M. W. Wong, C. Gonzalez, J. A. Pople, *Gaussian 03, Revision D.02*, Gaussian, Inc., Wallingford, CT, **2004**.
21. G. L. Miessler, D. A. Tarr, *Inorganic Chemistry*, Prentice-Hall, London, **1999**, pp. 452.
22. (a) C. Laurence, J. F. Gal, *Lewis Basicity and Affinity Scale*, Wiley-VCH, New York, **2010**; (b) R. G. Pearson, J. Songstad, *J. Am. Chem. Soc.* **1967**, 89, 1827.
23. (a) S. S. Zumdahl, S. A. Zumdahl, *Chemistry*, 8th ed., Brooks Cole, Belmont, CA, **2008**; (b) W. H. Brown, C. S. Foote, *Organic Chemistry*, 4th ed., Brooks Cole, Belmont, CA, **2005**.

